JOURNAL OF GEOPHYSICAL RESEARCH, VOL. 101, NO. B6, PAGES 13,869–13,882, JUNE 10, 1996

Geoelectric signals in China and the earthquake generation process

Jean J. Chu,[1] Xietai Gui,[2] Jingan Dai,[2] Chris Marone,[3]
Marc W. Spiegelman,[4] Leonardo Seeber,[4] and John G. Armbruster[4]

Abstract. We present original apparent resistivity records for stations located in the Chinese provinces of Hebei and Sichuan, along with seismicity patterns, fault maps, and limited hydrologic data. These records are part of a 30-year database of geoelectric signals that have been recorded in China by a nationwide network of more than 100 stations set up by the State Seismological Bureau of the People's Republic of China. The database includes the time period during which the *M* 7.8 1976 Tangshan and *M* 7.2 1976 Songpan earthquakes occurred. Resistivity data recorded in and around the epicentral region of the Tangshan event show coherent changes, both temporal and in areal distribution, years and months before and after the earthquakes. A regional change in water table occurred more than 3 years prior to the Tangshan earthquake. The resistivity and water table signals appear to correlate in the 2- to 3-year period prior to the earthquake. Rainfall records from the region around Tangshan, extending to the cities of Beijing and Tianjin, do not appear to account for the resistivity changes. Regional seismicity and active fault patterns in north China indicate that deformation occurs mainly along the borders of large tectonic blocks. The source region for the geoelectric signals appears to lie within a large shear zone, at the edge of a tectonic block undergoing rotation. The Tangshan epicentral area is thus only part of a larger zone of deformation. We suggest that dilational strain associated with the opening of fractures may lower resistivity and water table. For shallow crustal depths, such as those monitored by the Chinese geoelectric network, dilation and resistivity changes are expected to begin at stress levels well below the peak values of the seismic cycle. Our study suggests that in some cases the areal extent of geoelectric signals may be significantly larger than that of the eventual earthquake source dimension. The Chinese geoelectric database offers an opportunity to improve our understanding of possible geoelectric precursors to earthquakes.

Introduction

Motivation and Purpose

On July 28, 1976, a magnitude 7.8 earthquake occurred directly beneath the Chinese city of Tangshan, causing the loss of over 240,000 lives. This catastrophe stunned China and the world [*Qian*, 1989; *Chen et al.*, 1988]. Tens of thousands of Chinese researchers, under the auspices of China's State Seismological Bureau, intensified their efforts, initiated in 1966, to monitor earthquake-related phenomena. As a result of their work, large databases have been compiled spanning nearly 3 decades and involving the fields of geophysics, geology, geodesy, geochemistry, the atmospheric sciences, and biology [*Zhao and Qian*, 1978; *Qian et al.*, 1984; *Chen*, 1987; *Chen et al.*, 1988; *Ma et al.*, 1989; *Mei et al.*, 1993]. Due to differences in language and in cultural perspective, however, opportunities have been rare for the international scientific community to work closely with these data.

[1]Institute of Geology, Chinese Academy of Sciences, Beijing.
[2]Center for Analysis and Prediction, State Seismological Bureau, Beijing.
[3]Department of Earth, Atmospheric, and Planetary Sciences, Massachusetts Institute of Technology, Cambridge.
[4]Lamont-Doherty Earth Observatory of Columbia University, Palisades, New York.

Paper number 96JB00793.
0148-0227/96/96JB-00793$09.00

Motivated by the need to better understand possible geoelectric precursors to earthquakes, we have studied apparent resistivity records and related data covering a period of 20 years and including the *M* 7.8 Tangshan and *M* 7.2 Songpan earthquakes. We present the original records, some of which are available to the international community for the first time, and assess issues such as (1) data resolution and consistency between signals at neighboring stations, (2) the size and character of changes associated with the mainshocks relative to variations during the interseismic period, and (3) whether changes in rainfall or other hydrologic factors can explain spatiotemporal variations in apparent resistivity prior to the Tangshan earthquake.

Background

Chinese earthquake scientists use the term geoelectric signals to refer to changes in the electrical behavior of Earth's crust over time. This term covers a range of electromagnetic phenomena and measurements [*Park et al.*, 1993], but in this paper we focus only on apparent resistivity signals. Geoelectric signals have been observed in many countries, and numerous reports have associated these signals with the occurrence of earthquakes [e.g., *Barsukov*, 1970; *Mazzella and Morrison*, 1974; *Sobolev*, 1975; *Yukutake et al.*, 1978; *Zhao and Qian*, 1978; *Varotsos and Alexopoulos*, 1984; *Gershenzon et al.*, 1989, 1993; *Gui et al.*, 1989, 1990; *Park and Fitterman*, 1990; *Park*, 1991, 1992; *Chu*, 1992; *Molchanov et al.*, 1992; *Park et al.*, 1993; *Madden et al.*, 1993; *Hayakawa and*

Fujinawa, 1994; *Zhao and Qian*, 1994; *Molchanov and Hayakawa*, 1995; *Fenoglio et al.*, 1995, *Yépez et al.*, 1995].

In 1966, following the M 7.2 Xingtai earthquake, the Chinese government established a multidisciplinary earthquake research program [*Chen*, 1987]. A national geoelectric network of more than 100 monitoring stations was established covering the accessible, seismically active regions of China (Figure 1) [*Chu et al.*, 1992]. During the last 3 decades, more than 30 earthquakes of magnitude greater than 6.0 have occurred within the monitored area, and case studies of geoelectric records have been done for some of the larger events [*Qian et al.*, 1983, 1990; *Qian et al.*, 1984; *Qian*, 1985; *Gui et al.*, 1987; *Ma et al.*, 1989; *Zhao and Qian*, 1994].

We reexamine selected original resistivity measurements, primarily from stations in the region of Beijing, Tianjin, and Tangshan (Figure 1), and compare them to geologic, seismic, hydrologic and meteorologic data in that region.

Tectonic Setting

Regional Setting

North China contains the three cities of Beijing, Tianjin and Tangshan. It lies between the latitudes of 32° and 42° N and stretches from longitude 106° E to the Yellow Sea (Figure 2). Cenozoic tectonic activity in north China is more intense than in the surrounding regions [*Ma*, 1989] as indicated by geologic and seismic data. Figure 2 delineates the major tectonic features of north China, which is dominated by Quaternary faults [*Ma*, 1989; *Ye et al.*, 1987; *Burchfiel and Royden*, 1991]. These fault zones surround stable areas such as the Ordos Plateau and the Shanxi Uplift, which have deformed relatively little in Quaternary time (Figure 2). The southern border of north China consists of the Qinling-Dabie Shan fault belt, where left-lateral strike-slip faulting predominates [*Mattauer et al.*, 1985; *Peltzer et al.*, 1985].

The seismicity of North China shows a concentration of activity in relatively narrow zones surrounding stable blocks (Figure 2). Focal mechanisms and geologic data [*Mattauer et al.*, 1985; *Peltzer et al.*, 1985; *Ma*, 1989; *Wang*, 1994] indicate a sense of slip on the block boundaries that is consistent with counterclockwise block rotation and with eastward motion of south China relative to northeast China (Figure 2).

Three-City Area

Numerous large faults dissect the Beijing-Tianjin-Tangshan region [*Shao et al.*, 1989; *Zheng and Ma*, 1991]. The orientations of these faults differ, and three main fault sets can be distinguished: northeast, northwest, and east-west (Figure 3). Field investigations and drilling reveal that the most active group at present is the NW fault system [*Zheng and Ma*, 1991]. This system of densely clustered faults forms a tectonic zone 20-30 km wide that extends through the cities of Zhangjiakou, Huailai, Beijing, Ninghe, and Yantai (Figure 3).

The NW trending faults are steeply dipping normal and reverse faults that show remarkable Cenozoic activity [*Zheng and Ma* , 1991] (Figure 3). A series of basins occur near mapped fault terminations (Figure 3) and drill-hole data indicate that thicknesses of these Quaternary deposits locally exceeds 800 m [*Zheng and Ma*, 1991]. On the basis of the characteristics for

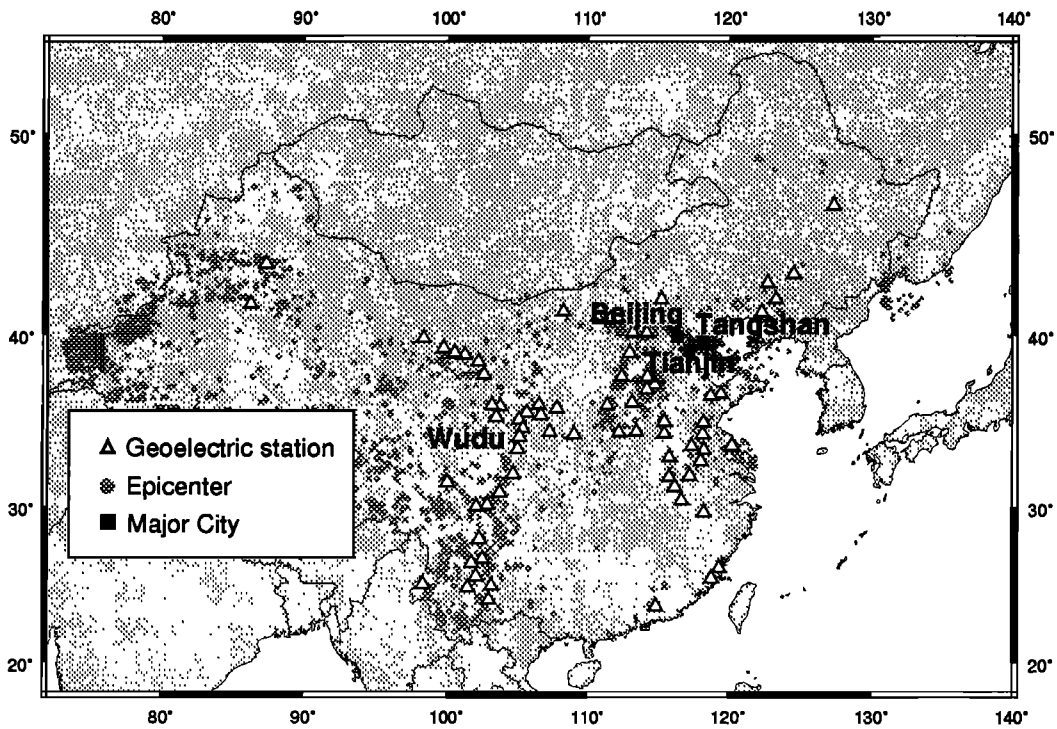

Figure 1. Map of China's geoelectric network and seismicity for the period 1966-1991. Epicenters are plotted for events of magnitude ≥ 2 in north China and $M \geq 5$ for the rest of the country (data sources are as follows: for north China, Beijing Seismic Network Z. Ma personal communication, 1991); elsewhere, preliminary determinations of epicenters compiled by U.S. Geological Survey, 1990. The M 7.2 1976 Songpan earthquake occurred near the city of Wudu.

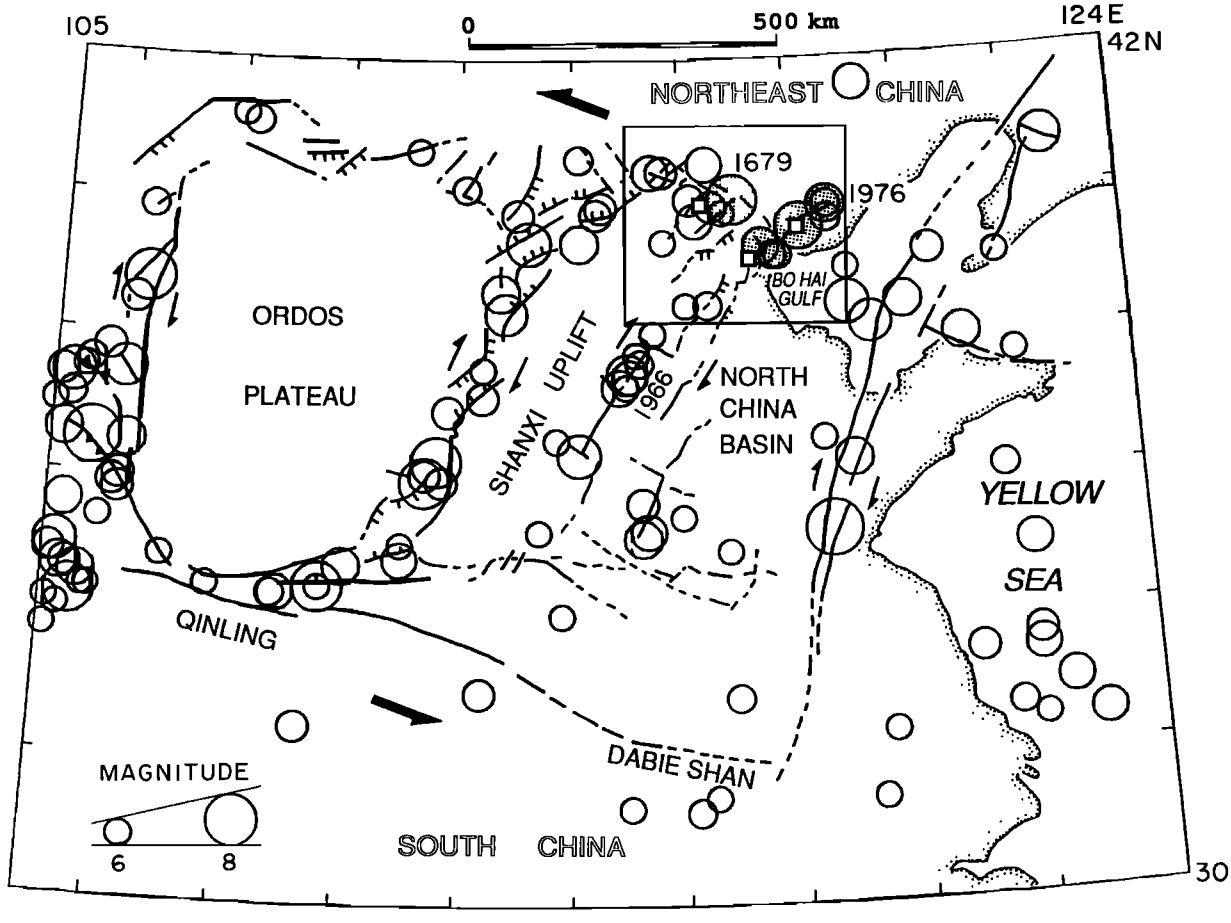

Figure 2. Map of North China showing major faults and seismicity. Northeast-southwest trending Quaternary faults bound relatively stable blocks within a NW trending, regional zone of sinistral shear (heavy arrows). Barbs and ticks indicate hanging wall of thrust and normal faults. Epicenters are plotted for $M \geq 6$ earthquakes during the last millennium (data are believed to be complete for $M \geq 8$). Shaded circles show 1679 Pinggu (M 8) and 1976 Tangshan earthquakes. The box in that region indicates the area of Figure 4, which shows the dense network of stations in the three-city region of Beijing, Tianjin, and Tangshan (white squares).

the NW tectonic zone, *Zheng and Ma* [1991] suggest that motion along this zone involves both shear displacement of the entire tectonic zone and nonhomogeneous rotation of individual blocks.

Seismic activity along this NW zone is intense (Figure 2). From historical records, 18 $M \geq 6$ earthquakes have occurred there over the last several millennia, including one $M \approx 8$ and four $M \geq 7$ [*Gu*, 1983]. The strongest, the Sanhe-Pinggu earthquake of 1679, occurred in the central section of this zone, making the Zhangjiakou-Yantai tectonic zone the best known active belt of strong earthquakes in the northern part of north China [*Zheng and Ma*, 1991]. In contrast, the region just north of the Zhangjiakou-Yantai tectonic zone shows a marked absence of seismic activity for earthquakes of $M \geq 6$ (Figures 1 and 2).

Resistivity Measurements

Method

The Chinese national geoelectric network (Figures 1 and 4) employs active source resistivity and self-potential measurements [*Qian et al.*, 1990]. This paper discusses apparent resistivity measurements made using active Schlumberger arrays. Each geoelectric station has at least two orthogonal, modified Schlumberger arrays (Figure 5a) composed of pairs of current (AB) and potential (MN) electrodes permanently buried at a depth of 1.5-2 m. Currents of 1-5 A are used, and connecting wires use dedicated telephone poles to avoid leakage to the ground and to minimize wire damage from ground movement during earthquakes. The current electrodes are separated by 1-3 km and potential electrodes are 200-500 m apart, resulting in a maximum penetration depth of 1 km [*Qian and Zhao*, 1992]. Unlike the standard use of the Schlumberger array for sounding and profiling, each array configuration is stationary. The sites thus monitor apparent resistivity variation over time.

Many of the stations have been in operation since the late 1960s, and the time period 1970 to 1990 includes both technical improvements and routine maintenance. Recently, data collection has been automated. For the time period we focus on, data were primarily read manually. Five to twelve resistivity measurements are made per day per array line. These are taken at regular intervals, except for one gap during the early morning hours. Each measurement is the average of at least five repeated readings. Thus in 1 day, 25 to 60 resistivity measurements are taken per array line. Every 24 hours a daily averaged value for each line is telegraphed to the Center for

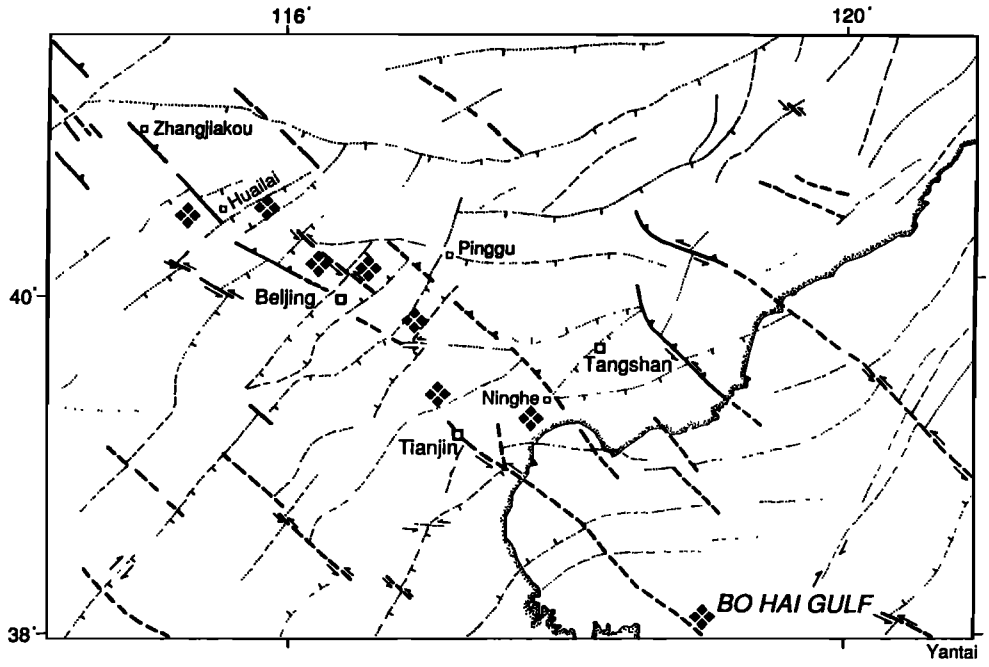

Figure 3. Quaternary and Neogene faults in and around the Beijing-Tianjin-Tangshan region (data from *Ma* [1989], *Ma et al.* [1989], *Shao et al.* [1989], and *Zheng and Ma* [1991]). Thin dotted lines indicate faults belonging to the NE-SW and E-W trending fault systems. Tick marks indicate dip directions. Thicker lines are faults related to the NW trending regional tectonic zone (see Figure 2). Checkered symbols indicate Quaternary basins; from northwest to southeast, names and thicknesses (based on drill-hole data) are Huailai (500 m), Yanqing (800 m), Machikou (600 m), Beiqijia (800 m), Xiadian (600 m), Wuqing (800 m), Ninghe (800 m), and Bozhong (greater than 800 m). Data are from *Guo et al.* [1982] and B. Zheng (personal communication, 1994). The city of Yantai is off the map to the southeast.

Analysis and Prediction in Beijing and logged in a station record book. We used the original measurements as recorded in these books and reported as monthly and daily averages. These books also include detailed notes on station maintenance and changes to instruments and array lines. The station books represent the dedicated effort of workers at the individual stations and at the Center for Analysis and Prediction of the State Seismological Bureau of China and form the basis for many published studies [e.g, *Zhao and Qian*, 1978, 1994; *Qian et al.*, 1984; *Chen*, 1987; *Ma et al.*, 1989; *Qian et al.*, 1990; *Zhao et al.*, 1991; *Qian and Zhao*, 1992; *Mei et al.*, 1993; *Park et al.*, 1993; *Madden et al.*, 1993].

Resistivity Data From the Three-City Area

We examine individual station records and compare apparent resistivity changes for fourteen stations monitoring the three-city region of Beijing, Tianjin, and Tangshan (Figure 4). These stations are distributed over an area approximately 300 km in width.

General observations. One of the longest records of the Chinese database is that from Baodi station, 80 km WNW from the city of Tangshan (BD in Figure 4). This record contains more than 20 years of nearly continuous readings [*Zhao et al.*, 1991]. Figure 5 shows the data from Baodi station as monthly averages for the period 1970 to 1991 (Figure 5b) and daily averages for 1973 and 1974 (Figure 5c). Here and in the figures that follow, we use the December 1973 monthly averaged value as a baseline reference (dashed horizontal line) against which to compare temporal variations. Later, we normalize by this value to compare relative changes between the stations, which have apparent resistivities ranging from 10 to 200 Ωm.

Prior to 1974, monthly averages at BD show annual variations of ≤1 Ωm (Figure 5b). The most significant features in the 21-year record are the broad resistivity depression extending from 1974 to 1981 and the increase in seasonal variation from about 1983 on relative to the pre-1974 period. The daily data show that the onset of the broad resistivity drop begins in early 1974 and is characterized by higher-frequency variation, particularly during the period from April to June 1974 (Figure 5c).

Similar features are apparent in data from Changli station (CL in Figure 4) 70 km E of Tangshan (Figure 6a). Seasonal variations after 1977 are larger than those prior to 1976 [*Qian et al.*, 1988; *Qian and Zhao*, 1992]. The resistivity low, centered in mid-1976, begins gradually in early 1975 and shows a sharp decrease followed by a gradual recovery (Figure 6b). Figure 6c shows measurements taken six to twelve times per day at Changli station. The data show very little variation in the early part of July 1976 relative to the sharp drop which begins in mid-July.

Relation to large earthquakes. In the period 1970 to 1991 there were five M≥6 earthquakes within the Beijing-Tangshan-Tianjin region (shown as stars in Figure 4). These were the July 28, 1976, *M* 7.8 Tangshan event, its three principal aftershocks (July 28, 1976, *M* 6.2; July 28, 1976, *M* 7.1, November 15, 1976, *M* 6.9) and the May 12, 1977, *M* 6.2 earthquake [*Chen et al.*, 1988]. These were the only large earthquakes within 200 km of the geoelectric stations discussed here.

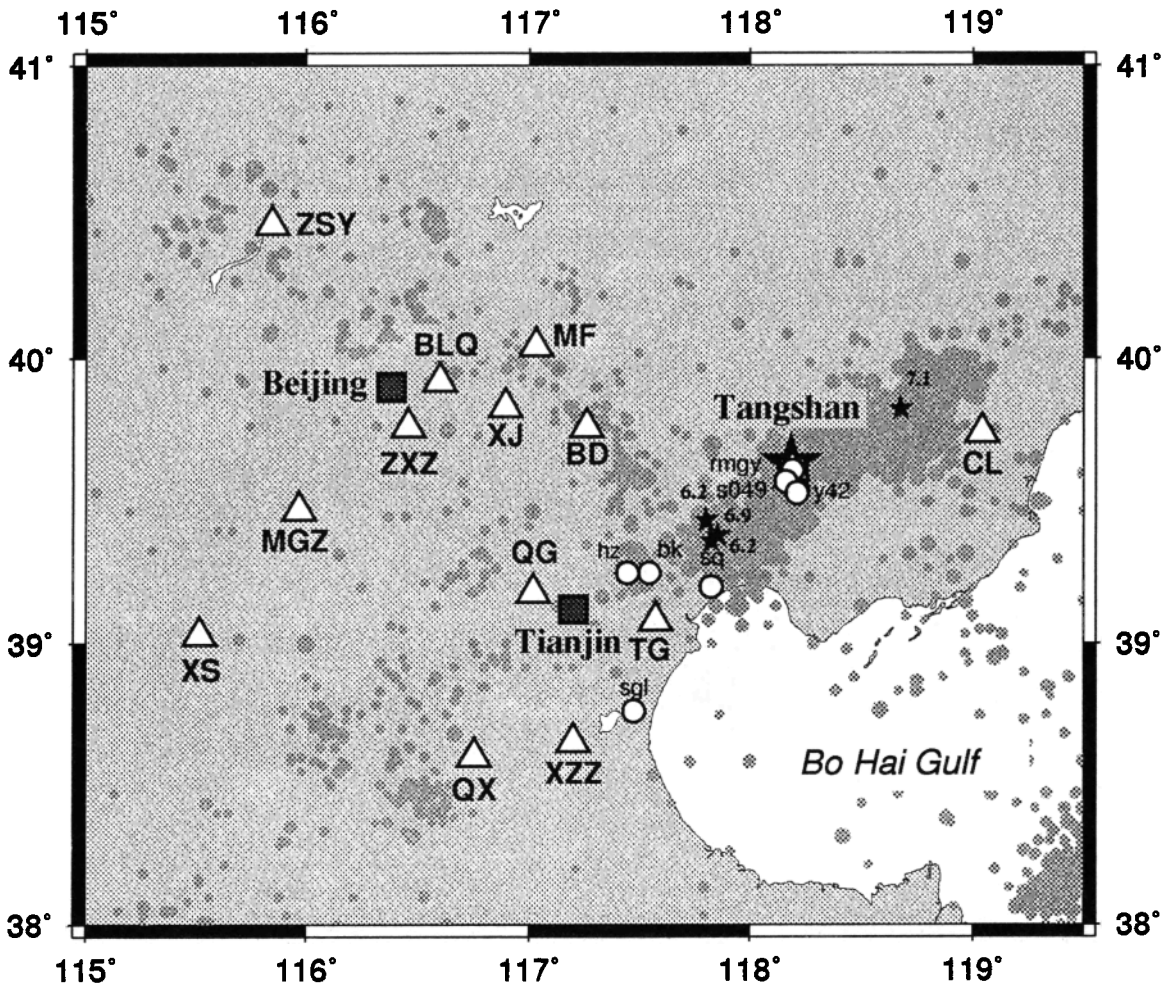

Figure 4. Network of geoelectric stations (triangles) and water wells (circles) for the Beijing-Tianjin-Tangshan region. Small gray dots indicate epicenters for earthquakes of $M \geq 2$ from 1970 to 1991 (Z. Ma, Centre for Analysis and Prediction, State Seismological Bureau, Beijing, written communication, 1991). Stars indicate epicenters of the major earthquakes ($M \geq 6$): M 7.8, July 28,1976; M 6.2, July 28, 1976; M 7.1, July 28, 1976; M 6.9, November 15, 1976; and M 6.2 May 12, 1977 [*Chen et al.*, 1988]. The Tangshan mainshock initiated at 11 km depth and ruptured bilaterally. Its aftershock zone extended from Tanggu (TG) station in the south to north of Changli station (CL).

At Baodi station, resistivity begins to drop more than 2 years before the 1976 Tangshan earthquake (Figure 5b). Resistivity values remain low from the time of the Tangshan mainshock to the end of 1977, the period containing the four largest aftershocks [*Chen et al.*, 1988]. Following these events, almost 3 years elapse before resistivity of the E-W array line returns to its pre-1974 level (Figure 5b). On the NS array line, resistivity values remain low through 1990.

At Changli station a long-term resistivity drop begins approximately 1.5 years before the Tangshan earthquake (Figure 6a). The slope of this downward trend changes rapidly and short-term variations appear about 2 weeks before the M 7.8 event (Figure 6). At higher frequencies (Figures 6b and 6c) the data form distinct troughs over a time period that includes the Tangshan mainshock and aftershocks. From January through June of 1976 the maximum variation is < 2.4 Ωm. In contrast, the variation in July reaches 16.0 Ωm, 6 times greater than during the previous 6 months. It takes 4 months for resistivity to return to its pre-July level (Figure 6b).

Regional data and time-space patterns. We focus now on the significance of the signals apparent at Baodi and Changli stations, addressing issues such as whether they are regional in nature and consistent in sign and magnitude with nearby stations, and their possible significance *vis-à-vis* the higher-frequency, short-term electrical signals studied by others [*Qian et al.*, 1983, 1990; *Qian*, 1985; *Bernard*, 1992: *Fraser-Smith et al.*, 1990; *Park*, 1991, 1992; *Molchanov et al.*, 1992; *Merzer and Klemperer*, 1993; *Madden et al.*, 1993; *Park et al.*, 1993; *Zhao and Qian*, 1994; *Fenoglio et al.*, 1995, *Yépez et al.*, 1995].

Figure 7 shows records from 10 stations in the Beijing-Tianjin-Tangshan region, arranged according to distance from the M 7.8 1976 Tangshan epicenter (see Figure 4). These stations include TS which was destroyed by the Tangshan mainshock, and MJG, a station established in an underground coal mine in January 1976. Data gaps represent intervals when data were not collected due to technical problems or maintenance. Several stations within 150 km of Tangshan

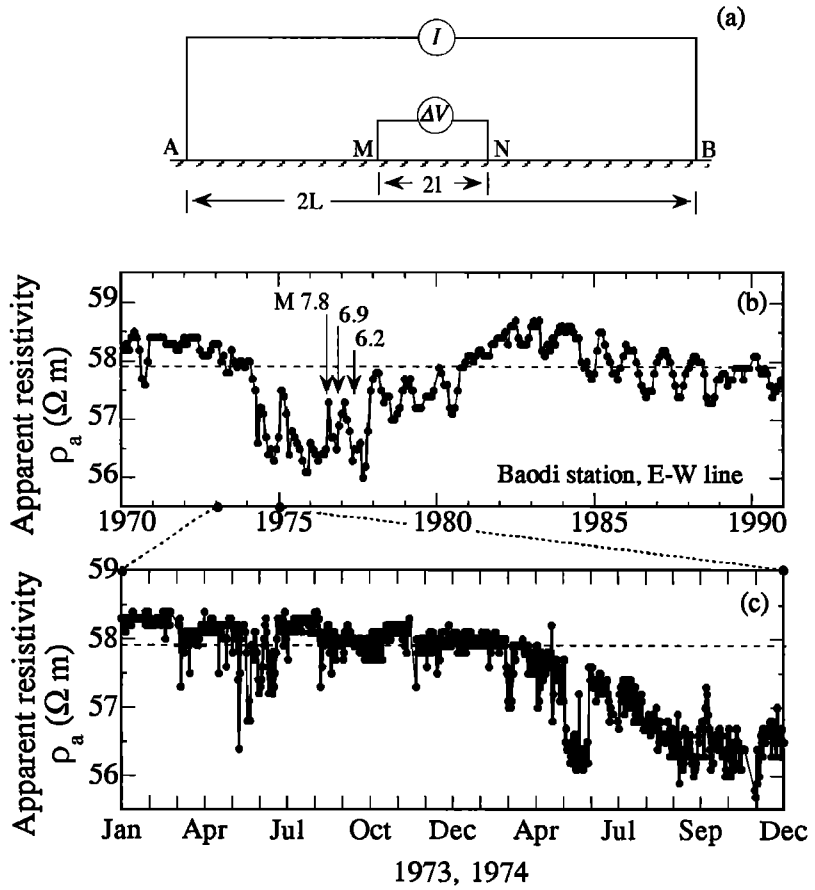

Figure 5. (a) Schematic diagram of the active Schlumberger resistivity array as used in the Chinese national network. In this configuration a field current I is applied through electrodes A and B, and the gradient potential ΔV is measured across points M and N. The ratio $\Delta V/I$ scaled by the array's geometric constant gives the apparent resistivity: $\rho_a = (\pi L^2/2l)(\Delta V/I))$, for $l \ll L$. For the Chinese network, L is 1-1.5 km, and l is 100-200 m. Each station has at least two orthogonal arrays, which are generally oriented NS and EW. (b) Monthly averages of apparent resistivity for EW line at Baodi station (BD in Figure 4) from 1970 through 1990. The dashed horizontal line indicates a reference value. Note the broad resistivity depression extending from 1974 to 1981. Arrows show time of the M 7.8 1976 Tangshan mainshock and aftershocks. (c) Detailed resistivity record for 1973 and 1974, showing daily averaged values. The onset of the broad resistivity depression apparent in Figure 5b begins in early 1974 and is characterized by a period of higher-frequency variation during the period from April to June 1974.

show decreasing resistivity beginning in about 1975, and others (e.g., BLQ) have an overall downward trend in resistivity (Figure 7). The decrease becomes more pronounced over time (e.g., records TS and ZXZ), appearing first at TS and later at BD and more distant stations. Several records show distinct changes at the time of the Tangshan earthquake (Figure 7).

To show spatiotemporal variations, we computed resistivity anomalies through time for each station and line. In Figure 8 the circles show the change in resistivity for the last month of each interval as a percentage of the December 1973 reference value. A spatial pattern of resistivity changes begins to develop in 1974. By the end of 1975, a region of reduced resistivity stretches from Tangshan southwest toward Tianjin and northwest to Beijing (Figure 8c). Stations more than about two source lengths from the eventual rupture zone appear to show increasing resistivity with time (solid circles, Figure 8). The well-developed spatial pattern of 1975 continues for at least 7 months and deepens within the three-city area. By June 1976, station TS in the city of Tangshan shows a -5% change in resistivity. One month later, TS is destroyed by the Tangshan earthquake. After the mainshock the areal extent of the resistivity anomaly is essentially unchanged (Figure 8e). Figure 8 suggests that the resistivity changes associated with the Tangshan earthquake are coherent over large areas.

The spatiotemporal relationship between resistivity changes and the Tangshan earthquake is given by the data and has been established in previous studies [*Qian et al.*, 1983; *Qian et al.*, 1984; *Ma et al.*, 1989; *Qian and Zhao*, 1992]. However, some debate exists as to whether the resistivity changes are related to the earthquake or to another factor. In the next sections we examine possible causes of changes in crustal resistivity, considering both tectonic and hydrologic effects.

Meteorologic and Hydrologic Data

Meteorologic Field Data

The Chinese electrical resistivity measurements are shallow and are therefore likely to be sensitive to changes in water table and rainfall. We obtained rainfall records for

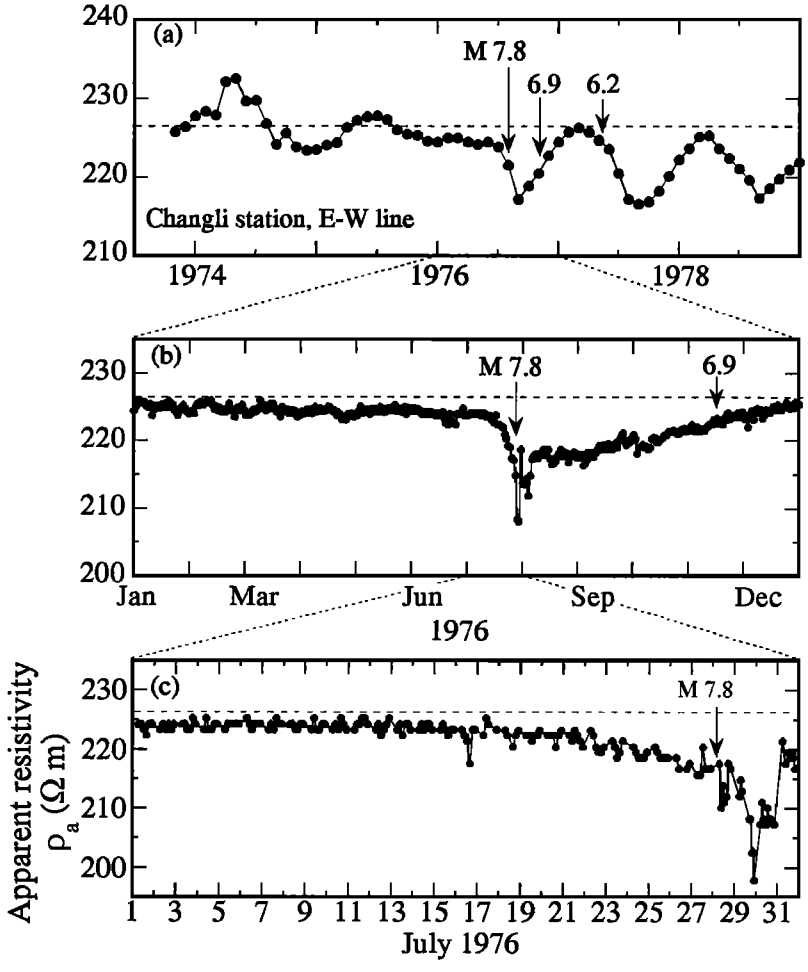

Figure 6. Apparent resistivity data for the EW array line at Changli station (CL), which is 70 km east of Tangshan (see Figure 4). Data are plotted at three different timescales: (a) monthly averages for the period November 1973 to July 1979; (b) daily averages for calendar year 1976, and (c) all available measurements for July 1976 (six to twelve times per day). Arrows indicate the time of the *M* 7.8 1976 Tangshan mainshock and aftershocks. Note that data are available for Changli prior to November 1973, however, we do not use them due to the numerous operational difficulties and electrode changes made during that time. The measurements are recorded to a precision of 0.1 Ωm, however, the data tend to cluster at discrete levels, indicating that the resolution is ≤1 Ωm. Note that for the first half of July the maximum variation is < 3 Ωm, while during the latter half it is as much as 24 Ωm. The changes prior to the Tangshan earthquake are therefore significantly above the short-term noise level.

meteorological stations in Beijing, Tianjin, and Tangshan for the period 1970 to 1981 (Q. Geng, personal communication, 1994). Figure 9 shows monthly averaged rainfall for the Beijing station and cumulative rainfall for all three stations. The records indicate a similar rainfall pattern for the tri-city area and apart from minor drier periods in 1972 and 1980, they indicate little change in the annual or cumulative pattern. Plotted with the rainfall data are apparent resistivity data from Baodi station, which is located roughly equidistant from each of the three cities.

Resistivity appears to have seasonal variations similar to the rainfall pattern, particularly after 1978 [*Qian et al.*, 1988; *Qian and Zhao*, 1992]. This similarity highlights the sensitivity of the resistivity measurements to seasonal changes in rainfall and indicates that when rainfall increases, resistivity decreases, with some lag (Figure 9). However, as indicated by the constant overall curvature of the cumulative records, there is nothing obvious in the rainfall pattern to explain the sharp resistivity drop in 1974 nor the prolonged reduction in resistivity at Baodi from 1974 to 1977 or at other stations in this region (see Figure 7).

Hydrologic Field Data

A groundwater observation network consisting of 400 wells was established in 1968 in the Beijing-Tianjin-Tangshan area. Most of these wells are shallow groundwater wells used by farmers, or pump wells reaching shallow aquifers. There are, however, a small number of deeper wells, of which about 30 are better confined and have long observation histories [*Mei*, 1982]. Most of these are located beyond the main aquifers quarried for irrigation, and their records are thus minimally affected by pumping [*Wang et al.*, 1984; C. Wang, personal communication, 1995].

Figure 10 shows water level data from three deep wells in the Tangshan area [*Mei*, 1982] along with the resistivity curves for the Tangshan geoelectric station. The well depths are in the

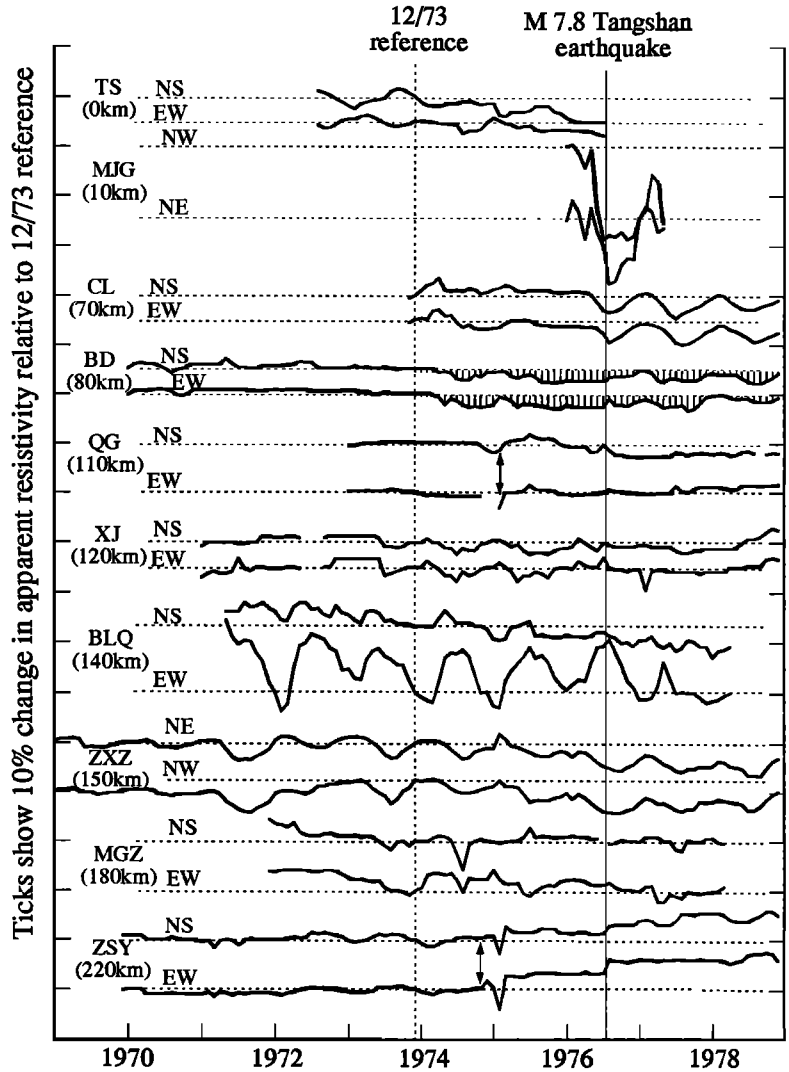

Figure 7. Relative apparent resistivity curves for ten stations monitoring the Beijing-Tianjin-Tangshan region (see Figure 4 for locations). Two curves at each station are shown, one for each orthogonal array direction. Vertical scale is percent change in resistivity. Each record has been normalized by its reference value in December 1973 and then offset vertically and arranged according to distance from the *M* 7.8 1976 Tangshan epicenter. Most stations show < 10% variation over the period 1969-1979. Note that station MJG is in an underground mine. Vertical lines between the BD reference lines and data show definition of resistivity anomaly as plotted in Figure 8. Small vertical arrows denote removal of minor offsets due to changes in electrodes and shortening of array lines. Data are from Center for Analysis and Prediction, State Seismological Bureau, 1980 and *Ma et al.* [1989]. Reference values are (in ohm meters) TS, 59.3 (NS), 54.4 (EW); MJG, 51.5 (NW), 43.0 (NE); CL, 195.2 (NS), 227.8 (EW); BD, 59.8 (NS), 57.9 (EW); QG, 11.3 (NS), 11.8 (EW); XJ, 24.0 (NS), 24.3 (EW); BLQ, 42.3 (NS), 37.9 (EW); ZXZ, 90.2 (NE), 74.1 (NW); MGZ, 18.1 (NS), 26.7 (EW); ZSY, 35.3 (NS), 40.4 (EW).

range monitored by the resistivity method. The three groundwater curves decrease by as much as 15 m. This downward trend begins in 1972 and becomes more pronounced in 1973. Resistivity at station TS generally decreases from 1974 onward, as indicated by the shading relative to the December 1973 reference values. Water table curves from wells around the city of Tianjin are similar in character to those of Tangshan (Figures 10 and 11). Changes in water level are less pronounced (from 1 to 10 m), but anomalous decreases begin from about 1972 (Figure 11).

A decrease in water level was first observed at the beginning of 1972 in Ninghe, midway between the cities of Tangshan and Tianjin, and gradually spread to Tangshan and Tianjin [*Wang et al.*, 1984]. The rate of decrease ranged from 30-40 cm/month near Tangshan to several centimeters per month in the suburbs of Tianjin. By the end of 1973 a large region of low water level was clearly defined [*Wang et al.*, 1984]. The regional drop in water table was initially attributed to heavy pumping in the Tianjin and Tangshan areas [*Wang et al.*, 1984]. However, this explanation was rejected when it was found that water level dropped in wells located outside the cones of influence of pumping and in wells that tapped aquifers below those utilized for pumping. Moreover, pumping records could not explain the behavior of the well water levels; e.g., despite heavy pumping immediately following the Tangshan earthquake water level did not drop (Figure 10) [*Wang et al.*, 1984; *C. Wang*, personal

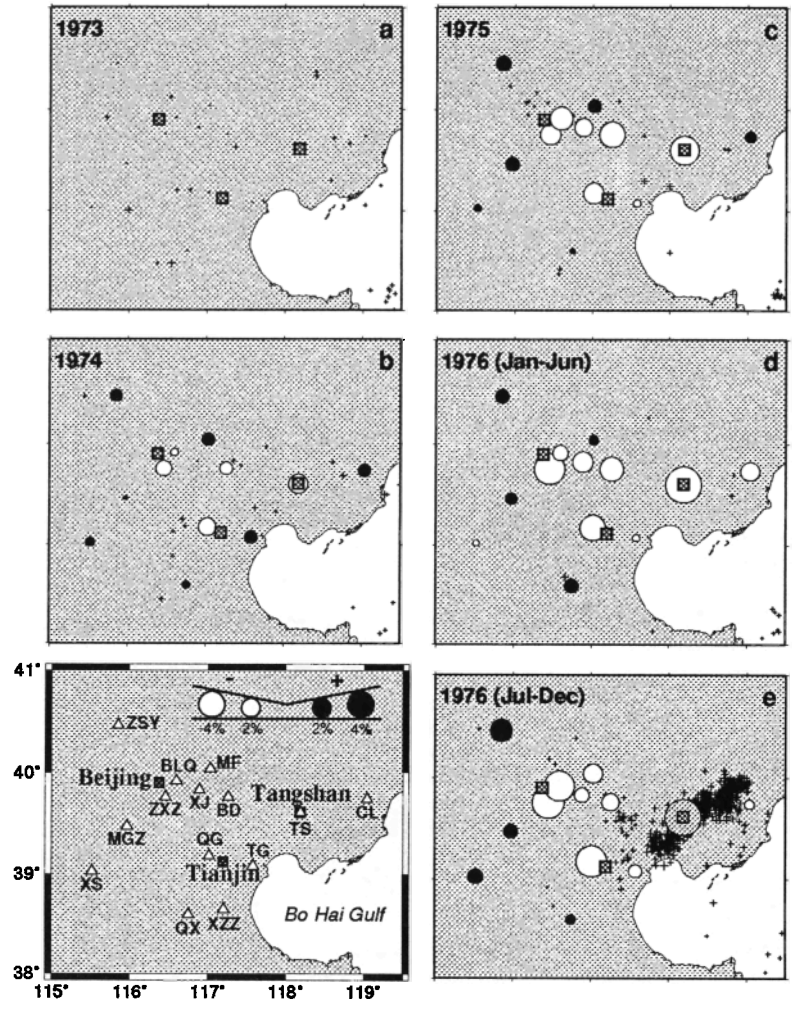

Figure 8. Spatio-temporal distribution of resistivity anomaly for the Beijing-Tianjin-Tangshan region. The bottom left panel gives geographic coordinates, station locations, and anomaly scale. Circle size represents the magnitude of the resistivity anomaly (solid circles, increased resistivity; open circles, decreased resistivity). Figure 8a to 8e show anomaly computed as the percentage change of the last month for the given period relative to the December 1973 reference value (see Figure 7). Earthquakes during each period are indicated by thin crosses (smallest cross, M 2.5). For the majority of stations, the resistivity values from the NS array lines are used. Note Figures 8a to 8d that a clear spatial pattern of lower resistivity develops in the eventual source region of the July 1976 mainshock. Figure 8e covers the time period including the M 7.8 Tangshan event. The resistivity value assigned to Tangshan station (shown by the gray circle) is taken from an underground station MJG, which survived and continued to record through the Tangshan mainshock. Aftershocks delineate the source region and mainshock rupture extent.

communication, 1995]. The regional change in water level noted by *Wang et al.* [1984] is similar in character to the changes in resistivity that appear in Figure 8 (C. Wang, personal communication, 1996).

Clear coseismic groundwater changes, coincident with the M 7.8 Tangshan mainshock, are seen in Figures 10 and 11. In the Tianjin region, SQ experiences an upwelling of water to become artesian [*Mei*, 1982]. Water level generally leveled out for about 1.5 years following the Tangshan earthquake, after which it decreased (Figures 10 and 11).

Discussion

The resistivity data show long-term temporal anomalies that do not appear to be explained by changes in rainfall. These anomalies are particularly interesting because they are consistent between neighboring stations and define a regional-scale areal anomaly prior to the Tangshan earthquake. The resistivity data appear to correlate with changes in water level and define a pattern that is consistent with the geologic and tectonic features of north China (Figures 2 and 3). The data are also consistent with strain measurements prior to the Tangshan earthquake, which indicated shortening over a 120-m baseline beginning in about 1975 [*Zhao et al.*, 1991; *Park et al.*, 1993]. Many of these observations have been known for some time, however, the problem has always been to develop a physical mechanism that accounts for the magnitude of the resistivity changes relative to strain and water level fluctuations and the temporal and spatial scales of the apparent precursory signals. While a full discussion based on the currently available data is beyond the scope of this paper, there are several points that can be addressed.

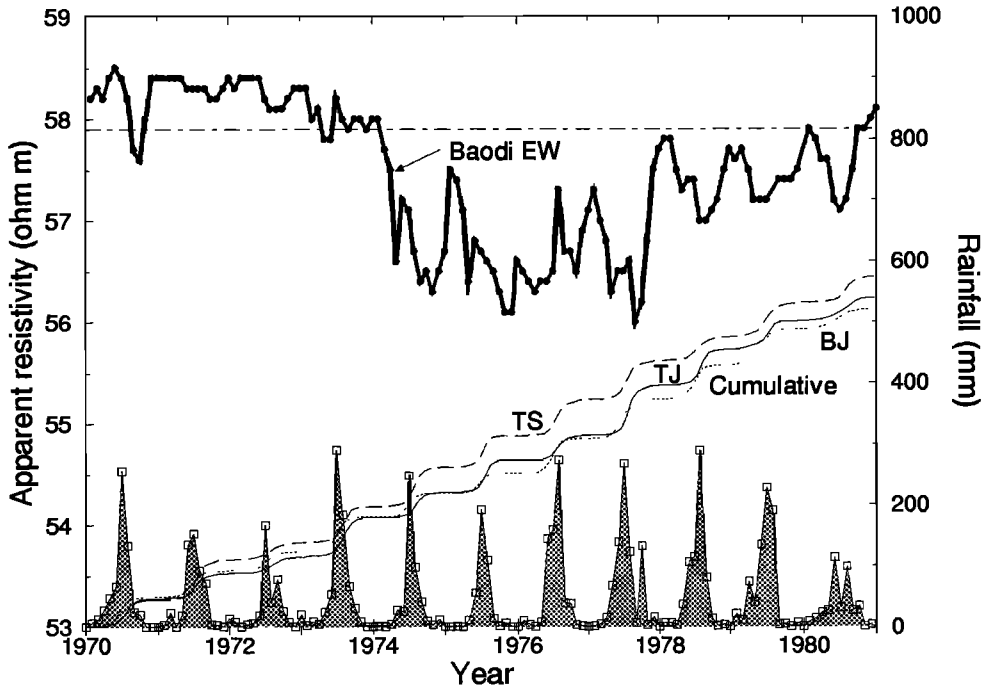

Figure 9. Comparison of rainfall data for meterological stations in Beijing (BJ), Tangshan (TS) and Tianjin (TJ) with resistivity data from station BD. The upper, bold curve shows monthly resistivity averages for the Baodi E-W line. The lower, shaded curve shows monthly rainfall for Beijing as open squares (in millimeters per month). Cumulative rainfall is given for each station (in centimeters). Note that the long-term resistivity anomaly beginning in about 1974 is not associated with any significant change in monthly or cumulative rainfall.

The combination of resistivity and hydrologic data presented above provides some constraints on possible mechanisms. If the reduction in resistivity were due to only an increase in fluid volume, the water table would be expected to rise, however, the opposite behavior is observed prior to the Tangshan earthquake (Figure 10). This result suggests a possible tectonic mechanism such as the dilation and fluid infiltration of cracks [e.g., *Scholz et al.*, 1973; *Wood and King*, 1993; *Gershenzon et al.*, 1993]. Dilatant cracks provide connected porosity, and flow into these conduits would lower resistivity and water table. Hydrologic effects of crustal strain have already been documented in several studies [e.g., *Roeloffs et al.*, 1989; *Wood and King*, 1993].

Moreover, results from laboratory experiments [e.g., *Brace et al.*, 1965, 1966, *Brace and Orange*, 1968; *Raleigh and Marone*, 1986] on both intact rock and simulated faults are qualitatively consistent with such a mechanism. They show that dilatancy and resistivity changes begin well before macroscopic failure. What is less appreciated is that among different synthetic fault experiments, there are large differences in behavior depending on the effective roughness and geometry of the fault (Figure 12). In laboratory faults for which the gouge thickness is large compared with the roughness of the bounding surface, dilation develops gradually with increasing shear strain compared to faults for which roughness is large. Fault gouge effectively reduces roughness and geometric complexity at wavelengths less than the gouge thickness. Since gouge thickness increases and geometric complexity decreases with accumulated fault offset [e.g., *Scholz*, 1987; *Wesnousky*, 1988, 1990], the laboratory data imply differences in the prefailure behavior of immature fault zones versus faults with wide gouge zones. Thus, rough geometrically complex fault zones such as in north China may show more dilation at lower shear strains than well-worked, gouged-filled faults such as the San Andreas. Clearly, more work needs to be done to test this speculation.

While a tectonic link between resistivity and groundwater is qualitatively appealing, the principal difficulty with such models and the current data is the requirement to produce apparent precursory signals at distances of the order of 100-200 km from the epicentral region. If the earthquake nucleation region is assumed to be small (of the order of 100 m or less, consistent with modeling studies and strain measurements [e.g., *Roy and Marone*, 1996; *Wyatt et al.*, 1994], (but see also *Ellsworth and Beroza* [1995]), then these scales become problematic because simple elastic dislocation models suggest that strain becomes immeasurable more than a few nucleation dimensions (or at most rupture dimensions) from the epicenter. This argument, however, is potentially misleading. We already know from the observed seismicity and geology that strain in north China is localized in complex fault zones along the edges of large (~300-1000km) tectonic blocks. The seismicity alone suggests that the natural scale of deformation is the block scale (or the scale of whatever drives the blocks) rather than the scale of the local rupture. We note that the geoelectric stations that show significant resistivity variations lie within this zone demarked by seismicity, and it is not inconceivable that stations 100 km from the eventual rupture could show coherent variations if strain is accommodated along the entire block edge in addition to the eventual rupture area. Such large-scale interactions have been suggested based on other types of data [e.g., *Keilis-Borok et al.*, 1988; *Silver and Valette-Silver*,

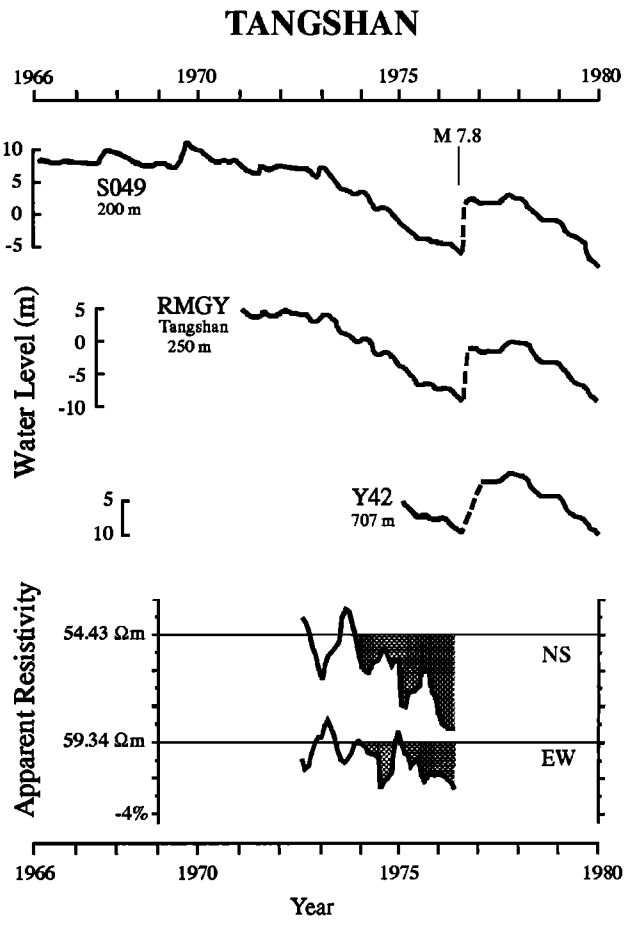

Figure 10. Comparison of water level data from three wells with resistivity data from Tangshan station. Well name and depth are given for each curve (see Figure 4 for well locations). Water level records are monthly averages of one reading/day [*Mei*, 1982]. For wells S049 and RMGY, which are monitored by the Ministry of Geology and Mineral Resources, the zero mark is sea level. The scale for Y42 (monitored by the State Seismological Bureau) refers to depth from Earth's surface to the well water level. Lower curves show normalized resistivity (monthly averages) at Tangshan station for the same period (shading indicates negative anomaly, starting from and relative to the December 1973 reference level). Note the correlation between the drop in water level, which begins in about 1973, the decrease in resistivity at TS, and the regional resistivity anomaly (Figure 8). A sudden increase in water level is associated with the *M* 7.8 1976 Tangshan earthquake.

1992; *Hill et al.*, 1993; *Press and Allen*, 1995]. Clearly, more work needs to be done from other regions to test and quantify this suggestion. Fortunately, an international program, under the auspices of the United Nations has been established to help coordinate further cooperative studies in this and other regions [United Nations, 1995].

Other tectonic settings can show resistivity behavior that is similar to that shown around Tangshan. As an example of other records in the Chinese geoelectric database, we show resistivity data from Wudu station in Sichuan province for 1976, which include the two *M*7.2 Songpan earthquakes (Figure 13). Wudu is located 1500 km to the west of Tangshan and lies at an altitude of about 1000 m (Figure 1). Its regional setting is compressional, in contrast to the three-city area, which is near sea level and in regional extension [*Burchfiel and Royden*, 1991]. Individual station records are compared for Wudu and Changli and show remarkable similarities (Figure 13). Both show a marked resistivity decrease a few months prior to the event. When plotted on the same timescale, the normalized relative resistivity changes show nearly identical temporal characteristics, with each showing an accelerating decrease prior to the earthquake followed by a gradual increase. The records suggest that the precursors to Tangshan are not unique and that resistivity signals, related in time and in space to earthquakes, may be monitored in various tectonic environments.

Conclusions

We present part of a 30-year database of geoelectric signals that have been collected in China. The resistivity and hydrologic data indicate temporal and spatial anomalies prior to the *M* 7.8 1976 Tangshan earthquake. The anomaly extends throughout the Beijing-Tianjin-Tangshan region, from 1973 through 1976. The data show resistivity changes and changes in well water level prior to the Tangshan earthquake. Changes

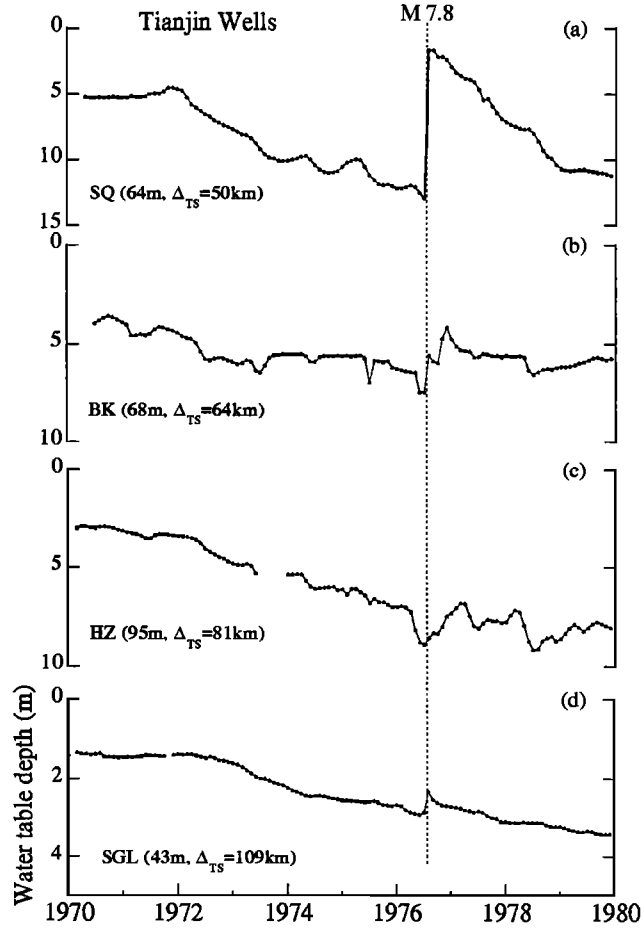

Figure 11. Water level records from 1970 to 1980 for wells around the city of Tianjin (data from C. Wang, (personal communication, 1995)). Each well is identified by its initials, depth of penetration, and distance Δ_{TS} from the M7.8 1976 Tangshan epicenter (see Figure 4 for well locations). The scale for each curve is relative to Earth's surface. At the time of the Tangshan earthquake, water gushed out of well SQ at the surface.

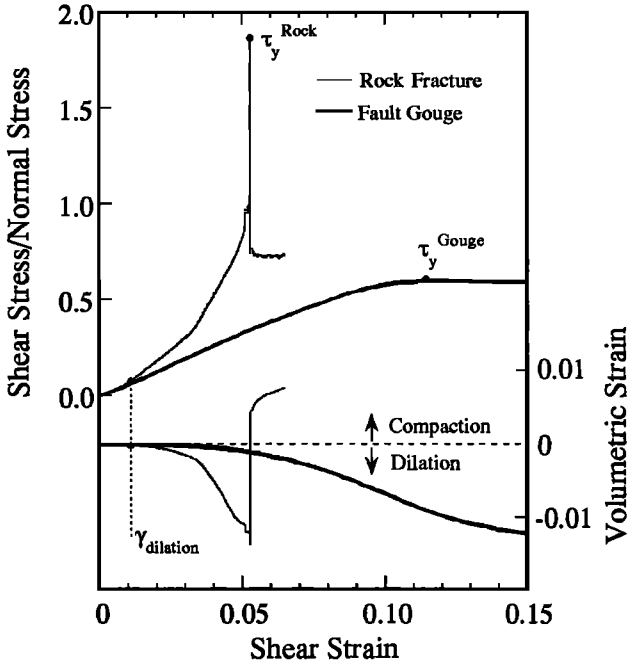

Figure 12. Shear strength and dilatant properties for a mated natural fracture (Westerly granite, max. roughness 5-6 mm) without fault gouge and a thick (3 mm) layer of granular fault gouge sheared between smooth bounding surfaces (roughness ≤50 μm). The experiments were done under room temperature and at constant normal stress. Normalized shear stress and relative volumetric strain (the zero level is arbitrary) are shown. The peak strength for each material is indicated by τ_y. The line $\gamma_{dilation}$ indicates the point at which dilation first occurs. For both cases, the onset of dilation occurs well before failure. For shear of the mated fracture, geometric complexity of the fault zone leads to abrupt changes in the dilatancy rate, and compaction accompanies failure. For the gouge layer, dilation occurs gradually and porosity reaches a roughly constant value upon failure. Data are from *Marone et al.* [1990] and *Marone* [1995].

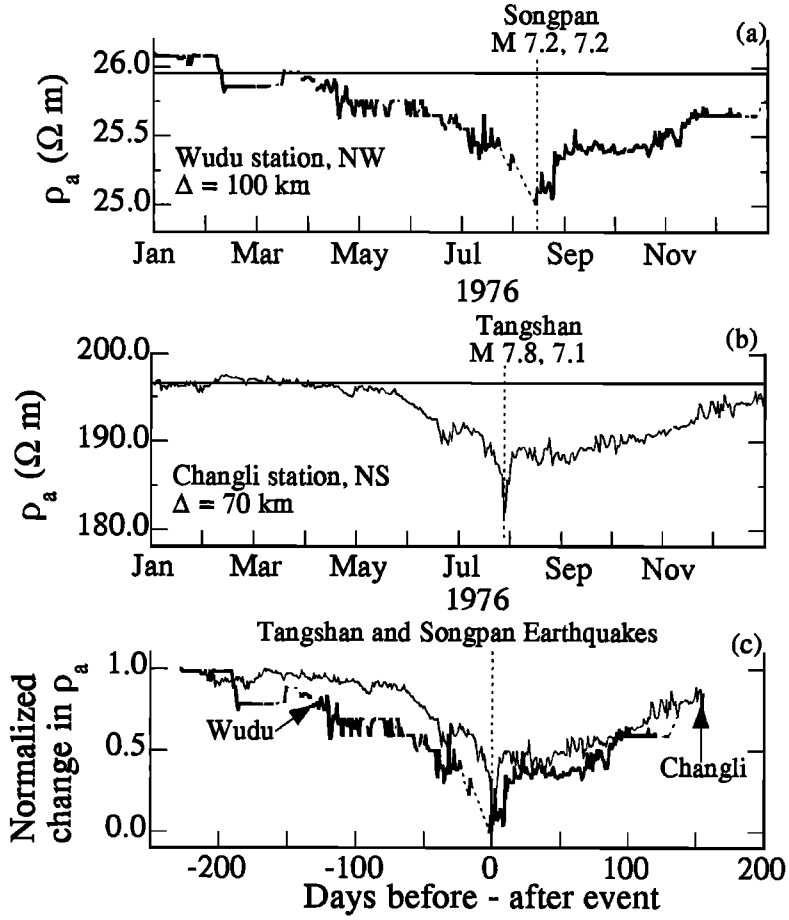

Figure 13. Comparison of resistivity records for two different sets of earthquakes and geoelectric stations. Wudu (Figure 1) is located 100 km from the Songpan earthquakes of August 16 and 23, 1976. Changli is situated 70 km from the *M* 7.8 Tangshan event of July 28, 1976. Records show daily ρ_a averages for 1976 along with the station reference level. (a) Data for NW array line at Wudu station. Gaps in the data are shown as dashed lines. (b) Data for NS array line at Changli station. Note the broad anomaly that begins 3-4 months before both the *M* 7.2 Songpan and the *M* 7.8 Tangshan earthquakes, respectively. (c) Data from Figures 13a and 13b are plotted as normalized relative changes on the same timescale, centered on the earthquake. Wudu is the heavy line. The resistivity anomalies have nearly identical temporal characteristics, with each showing an accelerating decrease prior to the earthquake followed by a gradual increase. Wudu station data are from *Gui et al.* [1987] and Z. Wang (personal communication, 1995).

in annual rainfall do not correlate with changes in resistivity or well water levels. The data are consistent with laboratory-based models in which crack dilation begin prior to macroscopic failure. Seismic and geologic data in north China indicate that large-scale stable blocks are bounded by zones of deformation. The resistivity and hydrologic precursors to the Tangshan earthquake may extend along these tectonic zones well outside the immediate epicentral region.

This study was motivated by data that are currently available to the international community. The data we present are a small fraction of the large multidisciplinary databases that exist in China. Further cooperation to examine, analyze, and synthesize these data sets is essential to test and expand our understanding of possible earthquake precursors and the nucleation process. The United Nations Global Program on the Integration of Public Administration and the Science of Disasters provides one avenue for such cooperation. Formulated by the United Nations Department for Development Support and Management Services, this program intends to focus first on the natural disaster of earthquakes.

Acknowledgments. We thank S. Zheng, Q. Geng, B. Zheng, and C. Wang for help in obtaining data. S. Uyeda, M. Hayakawa, and P. Wannamaker are thanked for thoughtful reviews and comments which greatly improved the manuscript. J.C. gratefully acknowledges guidance from B. Zheng, C. Wang, Y. Zhao, and F. Qian and encouragement and support from B.C. Burchfiel, L. Royden, T. Madden, C. Scholz, R. Boldi, and E. Wang. Major credit for this work belongs to the hundreds of Chinese professionals who devoted their lives to the development of geoelectric research in earthquake studies.

References

Barsukov, O. M., Relationship between the electrical resistivity of rocks and tectonic processes, *Izv. Acad. Sci. USSR Phys. Solid Earth*, no. 1, 84-89, 1970.

Bernard, P., Plausibility of long-distance electrotelluric precursors to earthquakes, *J. Geophys. Res.*, *97*, 17,531-17,546, 1992.

Brace, W. F., and A. S. Orange, Electrical resistivity changes in saturated rocks during fracture and sliding, *J. Geophys. Res.*, *73*, 1433-1445, 1968.

Brace, W. F., A. S. Orange, and T. R. Madden, The effect of pressure on the electrical resistivity of water-saturated crystalline rocks, *J. Geophys. Res.*, *70*, 5669-5678, 1965.

Brace, W. F., B. W. Paulding, and C. H. Scholz, Dilatancy in the fracture of crystalline rocks, *J. Geophys. Res.*, *71*, 3939-3953, 1966.

Burchfiel, B. C., and L. H. Royden, Tectonics of Asia 50 years after the death of Emile Argand, *Eclogae Geol. Helv.*, *84* (3), 599-629, 1991.

Chen, Y., K. Tsoi, F. Chen, Z. Gao, Q. Zou, and Z. Chen, *The Great Tangshan Earthquake of 1976*, 153 pp., Pergamon, Tarrytown, N.Y., 1988.

Chen, Z., Earthquake prediction research in China: Status and perspectives, *Earthquake Res. China*, *1*, 159-170, 1987.

Chu, J. J., A critical evaluation of Chinese earthquake electrical precursors and monitoring the high-risk areas of San Bernardino - Riverside, in *Proceedings of the International Workshop on Low Frequency Electrical Precursors*, edited by S. K. Park, *Rep. 92-15*, Inst. of Geophys. and Planet. Phys., Univ. of Calif., Riverside, 1992.

Chu, J. J., X. Gui, Y. Zhao, F. Qian, M. W. Spiegelman, L. Seeber, C. Scholz, and C. Marone, Earthquake prediction: An assessment of geoelectric signals in China (abstract), *Eos Trans. AGU*, *73*(43), Fall Meet. Suppl., 367, 1992.

Ellsworth, W. L., and G. C. Beroza, Seismic evidence for an earthquake nucleation phase, *Science*, *268*, 851-855, 1995.

Fenoglio, M. A., M. J. S. Johnston, and J. D. Byerlee, Magnetic and electric fields associated with changes in high pore pressure in fault zones: Application to the Loma Prieta ULF emissions, *J. Geophys. Res.*, *100*, 12,951-12,958, 1995.

Fraser-Smith, A. C., A. Bernardi, P. R. McGill, M. E. Ladd, R. A. Helliwell, and O. J. J. Villard, Low-frequency magnetic field measurements near the epicenter of the M_S 7.1 Loma Prieta earthquake, *Geophys. Res. Lett.*, *17*, 1465-1468, 1990.

Geological map of China, (in Chinese), Geological Press, Beijing, 1990.

Gershenzon, N. I., M. B. Gokhberg, A. V. Karakin, N. V. Petviashvili, and A. L. Rykunov, Modelling the connection between earthquake preparation processes and crustal electromagnetic emission, *Phys. Earth Planet. Inter.*, *57*, 129-138, 1989.

Gershenzon, N. I., M. B. Gokhberg, and S. L. Yunga, On the electromagnetic field of an earthquake focus, *Phys. Earth Planet. Inter.*, *77*, 13-19, 1993.

Gu, G. (E.), Catalogue of Chinese Earthquakes (1831 B.C. - 1979 A.D.) (in Chinese), Sci. Press, Beijing, 1983.

Gui, X., H. Guan, J. Dai, and M. Lu, Discussion on the observation and forecast indexes of the strong earthquake by geoelectrical apparent resistivity method (in Chinese), *South China Seismol. J.* *7*, 56-63, 1987.

Gui, X., H. Guan, and J. Dai, The short-term and immediate anomalous pattern recurrences of the apparent resistivity before the Tangshan and Songpan earthquakes of 1976, (in Chinese), *Northwest. Seismol. J.* *11*, 71-75, 1989.

Gui, X., H. Guan, J. Dai, and J. J. Chu, Earthquake prediction by electrical resistivity: China's twenty years of data (abstract), *Eos Trans. AGU*, *71*, 1825, 1990.

Guo, S., B. Zheng, and J. Xu, Jing-Jin-Tang diqu zhongshengdai yilai gouzao yinglichang tezheng, in *Dierjie Quanguo Gouzao Dizhi Xueshuhui Lunwenji Huixuanji, Disanjuan, Zhong-Zinshengdai Gouzao*, Beijing, 1982.

Hayakawa, M., and Y. Fujinawa (Eds.), *Electromagnetic Phenomena Related to Earthquake Prediction*, 677 pp., Terra Sci., Tokyo, 1994.

Hill, D. P., *et al.*, Seismicity remotely triggered by the magnitude 7.3 Landers, California, earthquake, *Science*, *260*, 1617-1623, 1993.

Keilis-Borok, V. I., L. Knopoff, I. M. Rotwain, and C. R. Allen, Intermediate term prediction of occurrence times of strong earthquakes, *Nature*, *335*, 690-694, 1988.

Ma, X. (E.), *Lithospheric Dynamics Atlas of China* (in Chinese and English), 68 maps, China Cartogr. Publi. House, Beijing, 1989.

Ma, Z., Z. Fu, Y. Zhang, C. Wang, G. Zhang, and D. Liu, *Earthquake Prediction: Nine Major Earthquakes in China (1966-1976)*, 332 pp., Springer-Verlag, New York, 1989.

Madden, T. R., G. A. LaTorraca, and S. K. Park, Electrical conductivity variations around the Palmdale section of the San Andreas fault zone, *J. Geophys. Res.*, *98*, 795-808, 1993.

Marone, C., Fault zone strength and failure criteria, *Geophys. Res. Lett.*, *22*, 723-726, 1995.

Marone, C., C. B. Raleigh, and C. H. Scholz, Frictional behavior and constitutive modeling of simulated fault gouge, *J. Geophys. Res.*, *95*, 7007-7025, 1990.

Mattauer, M., P. Matte, J. Malavieille, P. Tapponnier, H. Maluski, Xu Zhi Qin, Lu Yi Lun, and Tang Yao Qin, Tectonics of the Qinling Belt: Build-up and evolution of eastern Asia, *Nature*, *317*, 496-500, 1985.

Mazzella, A., and H. F. Morrison, Electrical resistivity variations associated with earthquakes on the San Andreas fault, *Science*, *185*, 855-857, 1974.

Mei, S. (E.), *The 1976 Tangshan Earthquake* (in Chinese), 459 pp., Seismol. Press, Beijing, 1982.

Mei, S., D. Feng, G. Zhang, Y. Zhu, X. Gao, and Z. Zhang, *Introduction to Earthquake Prediction in China* (in Chinese, with English preface, foreword, and table of Contents), 498 pp., Seismol. Press, Beijing, 1993.

Merzer, M., and S. L. Klemperer, Dilatant-conductive model for low-frequency magnetic-field precursors to the Loma Prieta earthquake using a precursory increase in fault zone conductivity (abstract), *Eos Trans. AGU*, *74*(43), Fall Meet. Suppl., 613, 1993.

Molchanov, O. A., and M. Hayakawa, Generation of ULF electromagnetic emissions by microfracturing, *Geophys. Res. Lett.*, *22*, 3091-3094, 1995.

Molchanov, O. A., Yu. A. Kopytenko, P. M. Voronov, E. A. Kopytenko, T. G. Matiashvili, A. C. Fraser-Smith, and A. Bernardi, Results of ULF magnetic field measurements near the epicenters of the Spitak (M_S = 6.9) and Loma Prieta (M_S = 7.1) earthquakes: Comparative analysis, *Geophys. Res. Lett.*, *19*, 1495-1498, 1992.

Park, S. K., Monitoring resistivity changes prior to earthquakes in Parkfield, California, with telluric arrays, *J. Geophys. Res.*, *96*, 14,211-14,237, 1991.

Park, S. K., Workshop on low-frequency electrical precursors to earthquakes, *Eos Trans. AGU*, *73*, 491-492, 1992.

Park, S. K., and D. V. Fitterman, Sensitivity of the telluric-monitoring array in Parkfield, California, to changes of resistivity, *J. Geophys. Res.*, *95*, 15,557-15,571, 1990.

Park, S. K., M. J. S. Johnston, T. R. Madden, F. D. Morgan, and H. F. Morrison, Electromagnetic precursors to earthquakes in the ULF

band: A review of observations and mechanisms, *Rev. Geophys., 31*, 117-132, 1993.

Peltzer, G., P. Tapponnier, Zhang Zhitao, and Xu Zhi Qin, Neogene and Quaternary faulting in and along the Qinling Shan, *Nature, 317*, 500-505, 1985.

Press, F., and C. Allen, Patterns of seismic release in the southern California region, *J. Geophys. Res., 100*, 6421-6430, 1995.

Qian, F., and Y. Zhao, Geoelectric precursors to the great Tangshan earthquake, in *Proceedings of the International Workshop on Low-Frequency Electrical Precursors*, edited by S. K. Park, *Rep. 92-15*, Inst. of Geophys. and Planet. Phys., Univ. of Calif., Riverside, 1992.

Qian, F., Y. Zhao, M. Yu, Z. Wang, X. Liu, S. Chang, Geoelectric resistivity anomalies before earthquakes, *Sci. Sini., Ser. B*, 26, 326-336, 1983.

Qian, F., Y. Zhao, and T. Xu, An analysis of the seasonal variation of disturbance in georesistivity, *Acta Seismol. Sini., 1*, 69-83, 1988.

Qian, F., Y. Zhao, T. Xu, Y. Ming, and H. Zhang, A model of an impending- earthquake precursor of geoelectricity triggered by tidal forces, *Phys. Earth Planet. Inter., 62*, 284-297, 1990.

Qian, G., *The Great China Earthquake*, 354 pp., Foreign Languages Press, Beijing, China, 1989.

Qian, J., Regional study of the anomalous change in apparent resistivity before the Tangshan earthquake (*M* 7.8, 1976) in China, *Pure Appl. Geophys, 122*, 901-920, 1985.

Qian, J., X. Gui, H. Ma, X. Ma, H. Guan, and Q. Zhao, Observations of apparent resistivity in the shallow crust before and after several great shallow earthquakes, in *Earthquake Prediction: Proceedings of the International Symposium on Earthquake Prediction*, pp. 145-155, Terra Sci., Tokyo, 1984.

Raleigh, B., and C. Marone, Dilatancy of quartz gouge in pure shear, in *Mineral and Rock Deformation: Laboratory Studies, Geophys. Monogr.*, Ser., vol. 36, pp. 1-10, AGU, Washington, D.C., 1986.

Roeloffs, E. A., S. S. Burford, F. S. Riley, and A. W. Records, Hydrologic effects on water level changes associated with episodic fault creep near Parkfield, California, *J. Geophys. Res., 94*, 12,387-12,402, 1989.

Roy, M. and C. Marone, Earthquake nucleation on models faults with rate and state dependent friction: effects of inertia, *J. Geophys. Res.*, in press, 1996.

Scholz, C. H., Wear and gouge formation in brittle faulting, *Geology, 15*, 493-495, 1987.

Scholz, C. H., L. R. Sykes, and Y. P. Aggrawal, Earthquake prediction: A physical basis, *Science, 181*, 803-810, 1973.

Shao, X., B. Zheng, and J. Zhang, New study results on crust structure, crust movement and conditions for earthquake preparation in the Yanshan region by converted waves, *Earthquake Res. China, 3*, 303-318, 1989.

Silver, P. G., and N. J. Valette-Silver, Detection of hydrothermal precursors to large northern California earthquakes, *Science, 257*, 1363-1368, 1992.

Sobolev, G. A., Application of electric method to the tentative short term forecast of Kamchatka earthquake, *Pure Appl. Geophys., 113*, 229-235, 1975.

United Nations, Guidelines for policy development and implementation for crises preparedness, *Publ. ST/SCD/Ser.E/32*, New York, Dec., 1995.

Varotsos, P., and K. Alexopoulos, Physical properties of the variations of the electric field of the Earth preceding earthquakes, I, *Tectonophysics, 110*, 73-98, 1984.

Wang, C., Y. Wang, H. Zhang, Y. Li, and S. Zhao, Characteristics of water-level variation in deep wells before and after the Tangshan earthquake of 1976, in *Earthquake Prediction: Proceedings of the International Symposium on Earthquake Prediction*, pp. 215-232, Terra Sci., Tokyo, 1984.

Wang, E., Late Cenozoic Xianshuihe/Xiaojiang and Red River fault systems of southwestern Sichuan and central Yunnan, China, Ph.D. thesis, 256 pp., Mass. Institut. of Technol., 1994.

Wesnousky, S. G., Seismological and structural evolution of strike-slip faults, *Nature, 355*, 340-343, 1988.

Wesnousky, S. G., Seismicity as a function of sumulative geologic offset: some observations from souther California, *Bull. Seismol. Soc. Am., 80*, 1374-1381, 1990.

Wood, R. M., and G. C. P. King, Hydrological signatures of earthquake strain, *J. Geophys. Res., 98*, 22,035-22,068, 1993.

Wyatt, F. K., D. C. Agnew, and M. Gladwin, Continuous measurements of crustal deformation for the 1992 Landers earthquake sequence, *Bull. Seismol. Soc. Am., 84*, 768-779, 1994.

Ye, H., B. Zhang, and F. Mao, The Cenozoic tectonic evolution of the Great North China: Two types of rifting and crustal necking in the Great North China and their tectonic implications, *Tectonophysics, 133*, 217-227, 1987.

Yépez, E. F. Angulo-Brown, J. A. Peralta, C. G. Pavia, and G. González-Santos, Electric field patterns as seismic precursors, *Geophys. Res. Lett., 22*, 3087-3090, 1995.

Yukutake, T., T. Yoshino, H. Utada, and T. Shimomura, Time variations observed in the earth resistivity on the Oshima volcano before the Izu-Oshima-Kinkai earthquake on January 14, 1978, *Bull. Earthquake Res. Inst.*, Univ. Tokyo, *53*, 961-972, 1978.

Zhao, Y., and F. Qian, Electrical resistivity anomaly observed in and around the epicentral area prior to the Tangshan earthquake of 1976 (in Chinese with English abstract), *Acta Geophys. Sini., 21*, 181-190, 1978.

Zhao, Y., and F. Qian, Geoelectric precursors to strong earthquakes in China, *Tectonophysics, 233*, 99-113, 1994.

Zhao, Y., F. Qian, and T. Xu, and Ming, Geoelectrical measurements from the experimental sites for earthquake prediction in China, paper presented at US-PRC Conference on Focused Earthquake Prediction Experiments, San Juan Bautista, Calif., Sept., 1991.

Zheng, B., and Z. Ma, Fault block tectonics in the northern part of North China and the structural detachment in the mid-lower crust, *Earthquake Res. China, 5*, 267-280, 1991.

J. B. Armbruster, L. Seeber, and M. W. Spiegelman, Lamont-Doherty Earth Observatory of Columbia University, Palisades, NY 10964.

J. J. Chu, Institute of Geology, Chinese Academy of Sciences, Beijing 100029; People's Republic of China.

J. Dai and X. Gui, Center for Analysis and Prediction, State Seismological Bureau, Beijing 100036; People's Republic of China.

C. Marone (corresponding author), Department of Earth, Atmospheric, and Planetary Sciences, Massachusetts Institute of Technology, Cambridge, MA 02139. (e-mail: cjm@westerly.mit.edu)

(Received April 20, 1995; revised February 29, 1996;
accepted March 6, 1996.)